Clinical and Translational Radiation Oncology 12 (2018) 21–27

Contents lists available at ScienceDirect

Clinical and Translational Radiation Oncology

journal homepage: www.elsevier.com/locate/ctro

Original Research Article

Verification of HE-based CTV in laryngeal and hypopharyngeal cancer using pan-cytokeratin

Hans Ligtenberg [a,*], Stefan M. Willems [b], Lilian N. Ruiter [b], Elise Anne Jager [a], Chris H.J. Terhaard [a], Cornelis P.J. Raaijmakers [a], Marielle E.P. Philippens [a]

[a] Department of Radiotherapy, University Medical Center Utrecht, PO Box 85500, 3508 GA Utrecht, The Netherlands
[b] Department of Pathology, University Medical Center Utrecht, PO Box 85500, 3508 GA Utrecht, The Netherlands

ARTICLE INFO

Article history:
Received 17 May 2018
Revised 6 July 2018
Accepted 9 July 2018
Available online 11 July 2018

Keywords:
Head and neck
Squamous cell carcinoma
Histopathology
Pan-cytokeratin
Target definition
HE

ABSTRACT

Background: For accurate target definition, we determined margins for the clinical target volume (CTV) for laryngeal and hypopharyngeal cancer in computed tomography (CT, 4.3 mm), magnetic resonance imaging (MR, 6.1 mm) and fluorodeoxyglucose (FDG)-positron emission tomography (PET, 5.2 mm). Previously, we used Hematoxylin-eosin (HE) stained whole-mount sections of total laryngectomy specimens as gold standard to define CTV margins. In the present study, we verified the HE-based tumor delineation with staining for pan-cytokeratin, specific for squamous cell carcinoma.

Methods: Twenty-seven patients with a T3/T4 laryngeal hypopharyngeal tumor were included. From each patient, a total laryngectomy specimen was obtained. Four subsequent 3-mm thick slices containing tumor were selected of which 4-μm thick whole-mount sections were obtained and stained with HE and for pan-cytokeratin CK-AE1/3. Tumors were microscopically delineated on both sections by an experienced head-and-neck pathologist. Tumor delineations were compared using the conformity index (CI) and the distance between both contours.

Results: The CI between HE-based and CK-AE1/3-based tumor delineations was 0.87. The maximum and 95th percentile (p95) extent of the HE-based tumor delineations from the CK-AE1/3-based tumor delineations were 1.7 mm and 0.7 mm, respectively. The maximum and p95 extent of the CK-AE1/3-based tumor delineations from the HE-based tumor delineations was 1.9 mm and 0.8 mm, respectively.

Conclusions: Histopathological assessment of tumor outline on standard HE-stained sections is comparable to microscopic tumor extent based on squamous cell specific pan-cytokeratin staining. Therefore, CTV margins based on HE based tumor contour will be adequate.

Introduction

In radiotherapy, accurate target definition is a crucial step to perform optimal radiation treatment of the tumor [1]. Inaccurate target definition might result in reduced local tumor control or increased side effects in case of overestimation of tumor size [2–4]. Currently, clinical CTV margins lack evidence and are mostly based on clinical experience. Therefore, further validation is needed using histopathology or detailed recurrence localization [5,6].

In current clinical practice, various imaging modalities such as computed tomography (CT), magnetic resonance imaging (MRI), and fluorodeoxyglucose positron-emission tomography (FDG-PET) can be used for gross tumor volume (GTV) delineation [7,8]. Due to the limited resolution of the images and partial volume effects, some microscopic tumorous tissue will not be visible using these imaging modalities. This microscopic tumor tissue, however,

Abbreviations: HE, hematoxylin-eosin; CTV, clinical target volume; CT, computed tomography; MRI, magnetic resonance imaging; FDG-PET, fluoro-deoxyglucose positron emission tomography; CI, conformity index; p95, 95th percentile; GTV, gross tumor volume; SCC, squamous cell carcinoma; CK-AE1/3, cytokeratin AE1/3 antibodies; TLE, total laryngectomy; HIER, heat-induced epitope retrieval; PBS, phosphate-buffered saline; DAB, diaminobenzidine; TME, tumor microenvironment.

* Corresponding author at: Department of Radiotherapy, Q00.3.11, University Medical Center Utrecht, PO Box 85500, 3508 GA Utrecht, The Netherlands.
E-mail addresses: h.ligtenberg@umcutrecht.nl (H. Ligtenberg), s.m.willems-4@umcutrecht.nl (S.M. Willems), l.n.ruiter-5@umcutrecht.nl (L.N. Ruiter), e.a.jager@umcutrecht.nl (E.A. Jager), c.h.j.terhaard@umcutrecht.nl (C.H.J. Terhaard), c.p.j.raaijmakers@umcutrecht.nl (C.P.J. Raaijmakers), m.philippens@umcutrecht.nl (M.E.P. Philippens).

https://doi.org/10.1016/j.ctro.2018.07.003
2405-6308/

needs to be incorporated in the treatment for effective radiotherapy, which is achieved by expansion of the GTV to a clinical target volume (CTV). Expansion of the GTV can be done either by including anatomical regions with high risk of microscopic spread or by concentric geometric expansion using CTV margins. Geometric expansion might be preferable, as a recent study indicated that this method is less prone to treatment plan variations between different radiotherapy departments [9]. CTV margins have been estimated based on either post hoc evaluation of local recurrences or on examination of the microscopic tumor extent in histopathological specimens [6,10–16]. The literature on the microscopic spread of primary head and neck tumors is sparse [17], but studies by Campbell et al. [10] and Fleury et al. [11] demonstrated that microscopic disease was mainly limited within 5 mm of the GTV defined macroscopically on whole-mount sections. For laryngeal and hypopharyngeal squamous cell carcinomas (SCCs) we concluded, in a previous study, that concentric geometric expansion of the GTV with these CTV margins should be 4–7 mm, dependent on the imaging modality used for GTV delineation [12]. These margins were derived by comparison of the GTVs delineated on CT, MRI and PET with the delineations of the microscopic tumor on whole-mount histopathological sections stained with hematoxylin-eosin (HE). These HE-based delineations were used as gold standard for CTV definition. The assumption was made that all microscopic tumor is visible on the HE stained sections as HE-staining is clinically used to assess excision adequacy by evaluating the presence of tumor at the margins of resection. Furthermore, HE-based tumor delineations show a low interobserver variation among pathologists, which indicates high precision of these delineations [18]. However, the question remained whether HE staining is sensitive enough for detecting all microscopic tumor growth. Therefore, verification of the HE-based tumor delineations is needed using another, more specific staining.

Squamous cells and accordingly SCCs are characterized by the expression of cytokeratins which can be immunohistochemically demonstrated using a pan-cytokeratin staining, such as cytokeratin-AE1/3 (CK-AE1/3), a cocktail of multiple antibodies directed against the epitopes of the most common keratins. Because of the high sensitivity of squamous cells for cytokeratin staining, it is particularly useful in clinical practice to identify or confirm the diagnosis SCC [19]. Therefore, the microscopic tumor visible on HE-stained sections might be intrinsically different from the microscopic tumor visible on sections stained for CK-AE1/3.

In this original study we use pan-cytokeratin CK-AE1/3 staining to investigate whether microscopic tumor delineations essentially differ from HE-staining in inclusion of all microscopic tumor tissue. This addresses the question whether HE based delineations adequately indicate the tumor for CTV margin definition.

Material and methods

Patient and tissue selection

In this study, 24 patients out of 27 patients included from an imaging-validation study were used in the present study [12]. These patients had primary cT3 (N = 4) or cT4 (N = 23) laryngeal or hypopharyngeal squamous cell carcinoma and were imaged with CT, MRI and FDG-PET prior to total laryngectomy (TLE). Tumor stage changed after pathology for one patient from cT3 to pT2, another patient from cT3 to pT4, and another patient from cT4 to pT3. The exclusion criteria for this study were contraindications for CT and for MRI contrast administration and insulin-dependent diabetes mellitus. Three patients were excluded after inclusion, because a tumor biopsy was performed between imaging and surgery, the tumor was fragmented during surgery, and one tumor was too large to fit on the whole-mount slides used for histopathology. The optimization of the specimen preparation process was completed in six patients prior to inclusion of the here reported 27 patients.

From the laryngectomy specimens of these patients, the complete tumor was sliced in axial histological tissue blocks of three millimeter thickness. For each patient, four successive tissue blocks containing tumor and the first cranial and first caudal tissue blocks without tumorous tissue (if available) were selected based on the corresponding HE-stained sections obtained for the imaging validation study [12]. In total, 108 central tissue blocks and 26 cranial and caudal tissue blocks were selected for further analysis, 28 cranial or caudal tissue blocks were missing.

Staining procedure

Microscopic slices were obtained from the selected paraffin-embedded tissue blocks. Per tissue block 10 consecutive 4 μm whole-mount sections were obtained, of which two were used in this study: one stained with HE and another one for CK-AE1/3.

The HE-staining was performed manually according to our clinical staining protocol. The sections were first deparaffinized and rehydrated, then stained with hematoxylin and eosin (Dako, Agilent Technologies, Santa Clara, California) and finally dehydrated and mounted. For immunohistochemical CK-AE1/3 staining, the sections were deparaffinized in xylene and rehydrated in 70% ethanol. Subsequently, the endogenous peroxidase activity was blocked by incubation in 5% solution of 30% hydrogen peroxidase in phosphate buffered saline (PBS) for 15 min. Heat induced epitope retrieval (HIER) was performed in 10 mM sodium citrate buffer (pH 6.0) at 80 °C in a stove for 30 min to reduce cartilage detachment. After HIER, the sections were rinsed with PBS and incubated in the primary antibodies CK-AE1/3 (1:250, Thermo Fisher Scientific Inc., Waltham, Massachusetts) for 60 min. After careful rinsing with PBS, the secondary antibody was applied for 30 min. After applying the secondary antibody and rinsing with PBS, diaminobenzidine (DAB) staining was applied for 10 min. The sections were counterstained with hematoxylin, air-dried and mounted in ClearVue™ (Thermo Fisher Scientific Inc.) (Fig. 1).

Analysis

An experienced head-and-neck pathologist microscopically delineated tumorous tissue on both the HE and CK-AE1/3 stained sections (Fig. 2). The manual delineations with a 0.6-mm thick permanent marker pen were performed independently and separately. The available cranial and caudal sections were checked for presence of tumor deposits by systematic evaluation of these sections using a microscope.

After the first contouring session, the sections were digitized and rigidly registered to each other by selecting manually 3–5 corresponding anatomical landmarks close to or in the tumor on both sections. The delineations were digitized by manually tracing the delineation of the tumor contour using an in-house developed software package [20]. If cartilage was lost during the staining process, resulting in discrepancies between the delineations on both stained sections, the delineations in the cartilage were adapted to either one of the stainings.

The maximum distance between the two delineations was determined. As the goal was to find intrinsic difference between the tumor contour on HE and CK-AE1/3, the larger distances (>2 mm) between the HE-based and the CK-AE1/3 based delineations were re-evaluated. If discrepancies were due to sample and human errors, i.e. tissue displacements, tissue loss or inattentiveness, these delineations were corrected. The revised delineations were used for further analysis.

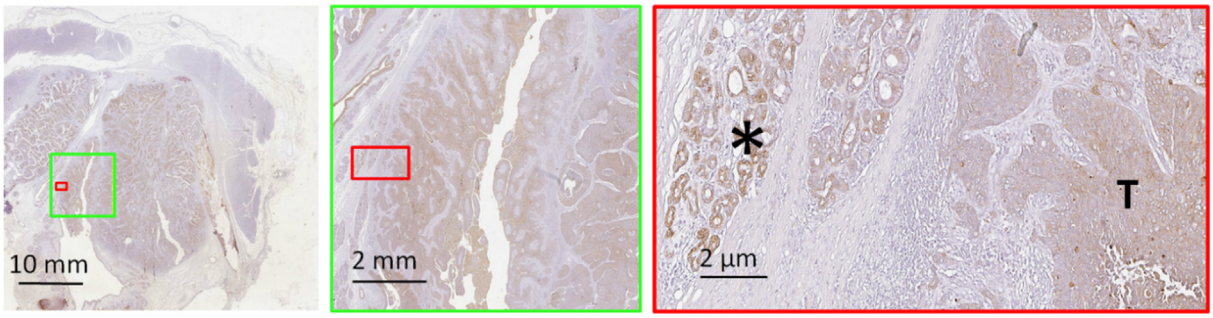

Fig. 1. CK-AE1/3 DAB-staining of a part of the tumor of patient 18 at different magnifications. The salivary gland is an internal positive control for the staining. *: salivary gland; T: tumor.

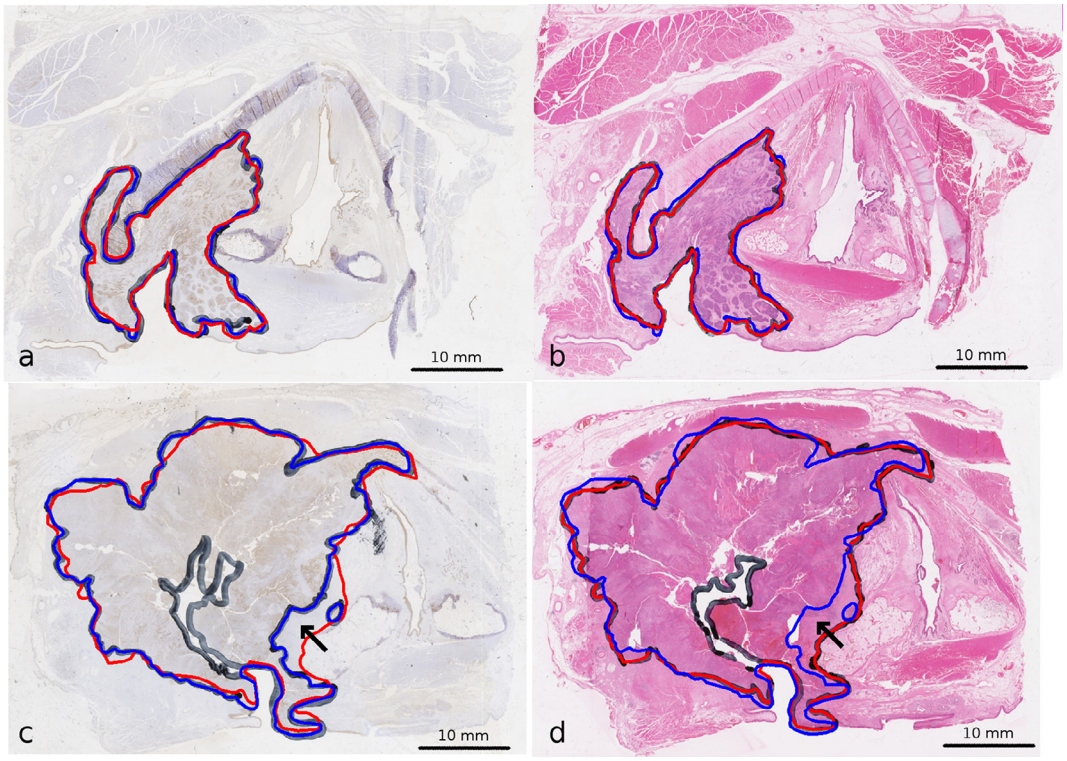

Fig. 2. A comparison of tumor delineations based on CK-AE1/3 (a,c) and HE staining (b,d) for a histology section of patient 7 (a,b) and patient 24 (c,d). The CI for between the HE-based delineation (red contour) and the CK-AE1/3-based delineations (blue contour) of the shown tumor is 0.89 and 0.88 for patient 7 and patient 24, respectively. For patient 24, the main difference is due to inclusion or exclusion of desmoplasia (arrow).

The conformity of both delineations was measured by the conformity index:

$$Conformity\ Index = \frac{A_{HE}A_{CKAE}}{A_{HE}A_{CKAE}}; \quad 0 \leqslant CI \leqslant 1 \tag{1}$$

$$with: \ A_{[staining]} = Area\ of\ staining,$$

with A_{HE} and A_{CKAE} the total delineated area per patient on HE and CK-AE1/3 stained section. A conformity of 1 indicates a perfect overlap of both delineations, and a conformity of 0 indicates no overlap between both delineations.

The CIs were compared with the expected variation of the CI due to the marker thickness for several tumor volumes. To assess the effect of the marker thickness on CI, the uncertainty on the CI was modeled as

$$CI_{expected} = \frac{A_{circle(r)}}{A_{circle(r+\Delta r)}} \tag{2}$$

with $A_{sphere}(r)$ the area of a circle with radius r and Δr the marker thickness. In this model we assume a circular shaped tumor delineation with an area that might vary between the inner and outer contour of the marker delineation. The correlation between the CI and the delineated tumor area was determined per patient.

Furthermore, a distance analysis was performed to describe the difference between the tumor delineations on both histological stained sections. The shortest distances from the contour of one staining to each position on the extending contour of the other staining were calculated per patient using the Hausdorff distance. This distance calculation was done for both the extent of the HE-based delineation to the CK-AE1/3-based delineation (HE-CKAE extent) and vice versa. From these distances the 95th percentile

distance (p95-distance) and the maximum distance were determined.

To account for tissue shrinkage between the macroscopic 3 mm thick slices and the histological sections, a 12% scaling factor was applied for the distance analysis, as a similar shrinkage was determined by Caldas-Magalhaes et al. [21].

Statistics

The Wilcoxon paired signed-rank test was used in all comparisons to determine significant differences, defined as a p-value lower than 0.05. To determine the correlation between tumor volume and CI, the Spearman rank correlation was determined. All statistical analyzes were performed using the statistics software package GraphPad Prism® 6.07 (GraphPad Software Inc., La Jolla, California).

Results

In total, 134 sections of 27 patients were examined after staining for HE and CK-AE1/3 They consisted of 108 sections containing tumor tissue and 26 cranial/caudal sections.

The median CI quantifying the conformity between the HE-based delineations and the CK-AE1/3-based delineations, was 0.87 (range 0.82–0.95) (Table 1). This result shows that the HE-delineation and CK-AE1/3 delineation agree in 87% of the delineated area (Fig. 3). A correlation of 0.71 ($p < 0.0001$) between delineated tumor area and CI existed. Frequently, variations between the delineation of both stainings could be attributed to inclusion or exclusion of tumor microenvironment (TME) containing no neoplastic tumor cells, but cancer associated fibroblast, tumor induced neo-vasculature and inflammatory cells attracted by the tumor (Figs. 3 and 4).

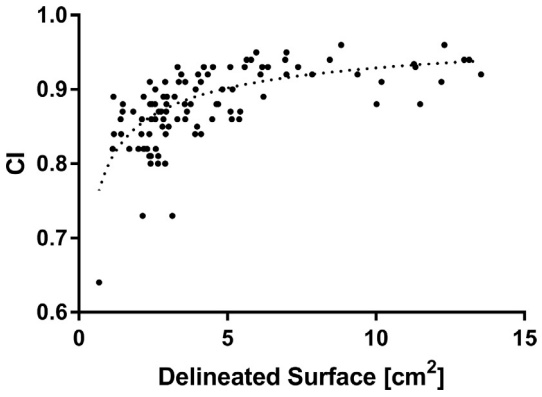

Fig. 3. The conformity index (CI) between the CK-AE1/3-based tumor delineation and the HE-based tumor delineation for 27 laryngeal carcinomas. The dashed line shows the simulated CI resulting from the marker thickness of 0.6 mm.

The expected CI due to the thickness of the marker on the overlap ranged from 0.76–0.94 (Fig. 3). The p95-distance and the maximum distance between both contours were calculated to determine how far the delineations deviate from each other (Fig. 4, Table 1). The median p95-distance of the extent of the HE-based delineations from the CK-AE1/3 based delineations (HE-CKAE extent) was 0.7 mm (range 0.3–1.3 mm) and the extent of the CK-AE1/3-based delineations from the HE-based delineations (CKAE-HE extent) was 0.8 mm (range 0.6–1.5 mm). The p95-distances were comparable for both stainings ($p = 0.19$) and were close to the pencil thickness used for delineation.

Table 1
Conformity parameters between HE-based and CK-AE1/3-based tumor delineations.

Patnr.	Tumor vol. [ml]	CI	HE-CKAE1/3 extent [mm]		CKAE1/3-HE extent [mm]	
			P95	Maximum	P95	Maximum
1	14.2	0.88	0.7	2.7	0.7	2.1
2	6.7	0.86	0.6	1.4	1.1	2.1
3	3.4	0.86	0.8	1.5	0.6	1.3
4	8.7	0.90	0.7	2.2	0.8	1.6
5	17.7	0.93	0.4	1.4	0.9	1.7
6	5.9	0.85	0.6	2.0	1.5	2.7
7	5.2	0.85	0.3	1.5	1.2	2.1
8	3.4	0.85	0.7	1.4	0.7	1.3
9	7.3	0.85	1.0	2.4	0.9	2.7
10	4.7	0.82	0.3	1.3	1.4	2.8
11	23.0	0.92	0.7	1.7	1.0	1.9
12	5.6	0.86	0.6	2.7	0.9	1.6
13	12.9	0.83	1.0	2.4	0.7	2.5
14	10.5	0.88	0.5	1.5	1.0	2.2
15	7.3	0.87	0.4	1.2	1.1	2.0
16	39.6	0.91	1.3	3.4	0.7	1.6
17	16.1	0.87	0.9	2.2	0.8	2.2
18	15.8	0.91	0.8	1.6	0.8	1.7
19	7.7	0.89	0.8	1.7	0.7	1.6
20	29.0	0.95	0.8	1.6	0.6	1.8
21	8.5	0.84	1.0	1.9	1.2	2.8
22	15.2	0.93	1.0	2.9	0.6	1.4
23	13.6	0.86	0.6	1.3	0.6	1.4
24	47.6	0.91	0.7	1.7	1.0	2.6
25	10.6	0.93	0.7	1.5	0.8	2.9
26	7.9	0.87	0.8	1.9	0.7	1.6
27	68.6	0.94	1.1	2.2	0.7	1.8
Median		0.87	0.7	1.7	0.8	1.9

CI: conformity index; HE-CKAE1/3 extent: the distance from the contour of tumor delineation on hematoxylin-eosin (HE) stained sections to the closest point on the contour of the tumor delineation on sections stained for pan-cytokeratine (CK-AE1/3). CKAE1/3-HE extent: the distance from the contour of the tumor delineation on sections stained for pan-cytokeratine (CK-AE1/3) to the closest point on the contour of the tumor delineation on hematoxylin-eosin (HE) stained sections; P95: 95th percentile of the measured distances from one contour to the other contour. Tumor volumes were published earlier in Ligtenberg et al. Radiother. Oncol. (2017).

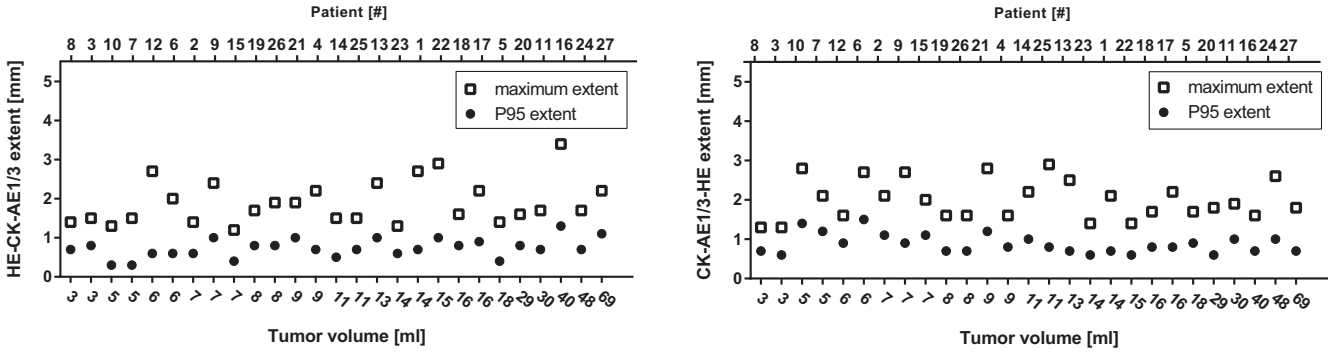

Fig. 4. The extent of both tumor delineations from each other. (a) The extent of the HE-delineation from the CK-AE1/3-delineation and (b) the extent of the CK-AE1/3-delineation from the HE-delineation. The maximum and 95th percentile (p95) extent for each patient are represented by an open square and a closed dot respectively.

The maximum extent was 1.7 mm (range 1.2–3.4 mm) for the HE-based delineation and 1.9 mm (range 1.3–2.9 mm) for the CK-AE1/3-based delineation and were not significantly different ($p = 0.31$) from each other.

In one of the sections of patient 22, an isolated microscopic tumor deposit, with a maximum diameter of 1.0 mm, was observed in both the CK-AE1/3 and the HE sections, at a distance of 4.3 mm from the main tumor bulk in the neighboring histological section (Fig. 5). This microscopic tumor deposit was surrounded by a layer of endothelial cells, indicating lymphogenic or hematogenous spread. The previously developed CTV margins of 4–6 mm incorporated this tumor deposit.

The cranial and caudal sections were microscopically examined for the existence of tumorous deposits, but no tumor deposits were observed in these sections.

Discussion

In this study, we evaluated the HE-based tumor delineations, used as a gold standard for CTV-margin definition, by comparison with CK-AE1/3-based tumor delineations. The CTV-margins for laryngeal and hypopharyngeal squamous cell carcinoma derived in our previous study were based on tumor delineations on histological sections stained with HE [12]. This is the first study which investigated the differences between HE-based tumor delineations and these based on immunohistochemical staining for cytokeratin. We observed that the HE-based tumor delineations were comparable to the CK-AE1/3-based tumor delineations within two millimeters. The variation between both tumor delineations, quantified using the conformity index (CI), was comparable to the interobserver variation on HE-based tumor delineations as determined by Jager et al. who reported a CI of 0.87 [18].

These results show that the added value of pan-cytokeratin staining for microscopic tumor definition was negligible and did not dictate adjustment of the previously developed CTV margins. Therefore, HE-based tumor delineations can be used in validation studies as gold standard target definition for laryngeal and hypopharyngeal carcinoma in radiotherapy.

No isolated microscopic tumor spread was observed near the main tumor bulk except for one lymphogenic-/hematogenous micrometastasis located within 4 mm from the main tumor bulk, which was visible on both HE and CK-AE1/3 stained sections.

The differences between CK-AE1/3 and HE based tumor delineations were small compared to the differences between HE based and clinical imaging based GTV delineations asfor CT and MRI the CI was 0.47 and 0.55, and the maximum extent was 4.6 mm and 4.3 mm [7,12,22], respectively. Effectively, the observer variations on imaging and histology were both part of these microscopic tumor extents, and thus taken into account in the derived CTV margins. Therefore, an additional margin for the pathological inter/intra-observer variation was unnecessary.

As generally, a correlation between CI and tumor volume was observed in our study, which is caused by the inherently higher sensitivity of the CI for variations in small volumes than for larger volumes. The tumor stage of the patients included in this study was predominantly T4, whereas usually patients treated with

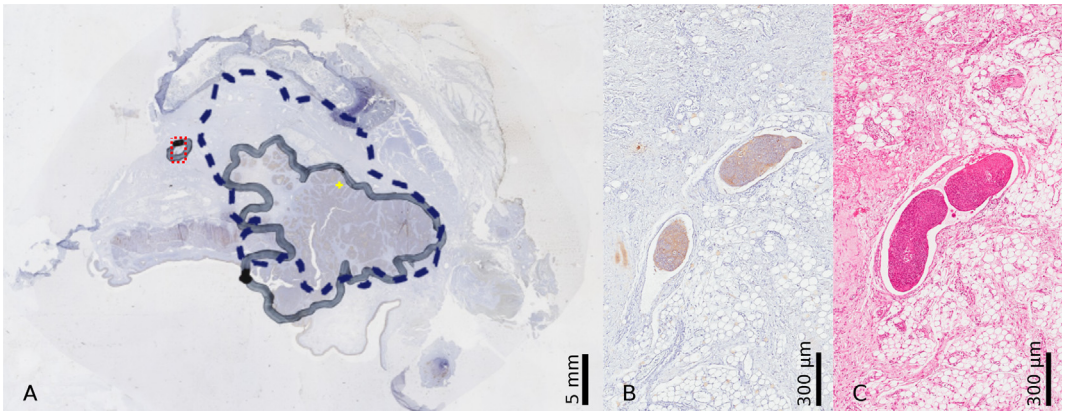

Fig. 5. The only section with a tumor deposit, observed both on the whole-mount sections stained for CK-AE1/3 and HE. (A) The delineation of the tumor on the CK-AE1/3 section (black line) and the delineation of the tumor on a neighboring section 3 mm apart (blue dashed line) are shown. The isolated tumor deposit is located closer to the main tumor delineated in the neighboring section than to the main tumor delineated in the section where the tumor deposit is detected. The tumor deposit (red dashed rectangle) is shown at larger magnification on the (B) CK-AE1/3 and (C) HE sections.

radiotherapy have lower stage tumors (T1b-T3). The lower stage tumors are typically smaller than the high stage tumors, and thus, this study might show higher CI than for tumors indicated for radiotherapy. The measured CI for the two types of tumor delineations was closely following the simulated CI calculated for a marker thickness of 0.6 mm. This suggests that the tumor delineations were similar and that delineation variation can partially be attributed to the physical marker thickness. Delineations of the tumor boundary can be considered to be different when the distance between the digitized delineations is larger than twice the marker thickness.

It is known that tumor delineation and even diagnosis of invasion into cartilage or bone is difficult on CT and MRI data [23,24]. We also found these discrepancies between HE and cytokeratin based delineations. The discrepancy in delineations for tumor invaded cartilage is in correspondence with the high interobserver variation for delineation of cartilage invasion on HE stained sections [18]. We observed that the tumor tissue was sometimes discontinuously infiltrating the bone marrow and that background staining was high in this area for CK-AE1/3; both might have resulted in the variation between HE and CK-AE1/3 based delineations in the cartilage.

Dissimilarities in delineation contour between HE and CK-AE1/3 might be attributed to varying inclusion and exclusion of TME at the border of the tumor. Whether TME should be included in the CTV, and thus needs to be irradiated, is subject of an ongoing debate. Currently the TME is seen as an important protector of malignant cells [25]; irradiation of the TME might therefore affect tumor proliferation. Clear delineation guidelines to include or exclude TME might have reduced the variation between HE based and CK-AE1/3 based tumor delineations, as the inclusion of TME was inconsistent, both on HE and CK-AE1/3 stained sections.

In several cases, staining for CK-AE1/3 was weak, which might be caused by dedifferentiation of tumors, which can reduce the amount of cytokeratin expressed in the tumor tissue, as was shown for cytokeratin-17 in oral SCCs [26,27]. As such, some dedifferentiated regions of the tumor were detected more easily on HE than on CK-AE1/3 stained sections.

In our study, we observed that when two dimensional (2D) sections were inspected, apparent isolated tumor deposits seemed to exist. However, when adjacent sections were taken into account, they appeared connected to the main tumor. Therefore, in general, to determine the existence of isolated tumor deposits, taking into account the three-dimensional tumor shape is of utmost importance in radiotherapy. However, when comparing tumor contours based on two different staining methods on sections less than 40 μm apart, small differences can be expected in tissue structure. Therefore, in this study, distance analysis was performed in the sectional plane only.

In this study, only patients with larynx and hypopharynx tumors indicated for surgery were included with a relatively high stage (T3/T4) compared to patients with T1b, T2 or T3 tumors who are typically indicated for radiotherapy. These tumors with a lower T stage as well as squamous cell carcinoma in other head-and-neck regions may present different tumor characteristics. We expect that the comparison of tumor contours on CK-AE1/3 and HE sections would be comparable to the higher T stage cases in the present study. Additionally, the question rises whether the CTV margins defined on the current study population might be transferred to other head-and-neck regions. As pattern of invasion and perineural growth in laryngeal cancer might be different from cancer in other head-and neck regions, transferring the CTV margins to these regions should be handled with caution [28].

Only a rigid registration of the stained section was performed in this study. However, deformable registration does not appear to be required, as the contours after rigid registration showed a high conformity.

Although we observed only one isolated tumor deposit in our study, single isolated tumor cells or very small tumor deposits might be below our detection level. However, it is questionable whether these very small tumor deposits and isolated tumor cells should be included in the primary tumor CTV, an elective radiation dose might be enough. Another question is which dose level is adequate for the CTV. As is discussed by Gregoire et al. [5] a two-level dose for the CTV might be implemented. For the near tumor CTV a high dose to adequately irradiate tumor tissue that is not included in the GTV, while at larger distance a lower dose level might be sufficient.

Conclusion

In conclusion, HE-based tumor delineations are comparable to CK-AE1/3-based tumor delineations in laryngeal and hypopharyngeal squamous cell carcinoma. Therefore, HE-based tumor delineations are a reliable standard to determine microscopic tumor extent for clinical target volume definition. Consequently, additional CK-AE1/3 staining is not necessary to accurately determine the microscopic tumor extent in validation studies.

Acknowledgement

This work was supported by the Dutch Cancer Society Grant UU 2011-5152 and UU 2011-5216.

Disclosure statement

No potential conflict of interest was reported by the authors.

Conflict of interest statement

None.

References

[1] Rasch C, Steenbakkers R, van Herk M. Target definition in prostate, head, and neck. Semin Radiat Oncol 2005;15:136–45. https://doi.org/10.1016/j.semradonc.2005.01.005.
[2] Vinod SK, Jameson MG, Min M, Holloway LC. Uncertainties in volume delineation in radiation oncology: a systematic review and recommendations for future studies. Radiother Oncol 2016;121:169–79. https://doi.org/10.1016/j.radonc.2016.09.009.
[3] Vugts CAJM, Terhaard CHJ, Philippens MEP, Pameijer FA, Kasperts N, Raaijmakers CPJ. Consequences of tumor planning target volume reduction in treatment of T2-T4 laryngeal cancer. Radiat Oncol 2014;9:195. https://doi.org/10.1186/1748-717X-9-195.
[4] Samuels SE, Eisbruch A, Vineberg K, Lee J, Lee C, Matuszak MM, et al. Methods for reducing normal tissue complication probabilities in oropharyngeal cancer: dose reduction or planning target volume elimination. Int J Radiat Oncol 2016;96:645–52. https://doi.org/10.1016/j.ijrobp.2016.06.2456.
[5] Grégoire V, Evans M, Le Q-T, Bourhis J, Budach V, Chen A, et al. Delineation of the primary tumour Clinical Target Volumes (CTV-P) in laryngeal, hypopharyngeal, oropharyngeal and oral cavity squamous cell carcinoma: AIRO, CACA, DAHANCA, EORTC, GEORCC, GORTEC, HKNPCSG, HNCIG, IAG-KHT, LPRHHT, NCIC CTG, NCRI, NRG Oncolog. Radiother Oncol 2018;126:3–24. https://doi.org/10.1016/j.radonc.2017.10.016.
[6] Apolle R, Rehm M, Bortfeld T, Baumann M, Troost EGC. The clinical target volume in lung, head-and-neck, and esophageal cancer: lessons from pathological measurement and recurrence analysis. Clin Transl Radiat Oncol 2017;3:1–8. https://doi.org/10.1016/j.ctro.2017.01.006.
[7] Jager EA, Ligtenberg H, Caldas-Magalhaes J, Schakel T, Philippens ME, Pameijer FA, et al. Validated guidelines for tumor delineation on magnetic resonance imaging for laryngeal and hypopharyngeal cancer. Acta Oncol 2016;55:1305–12. https://doi.org/10.1080/0284186X.2016.1219048.
[8] Leclerc M, Lartigau E, Lacornerie T, Daisne J-F, Kramar A, Grégoire V. Primary tumor delineation based on 18FDG PET for locally advanced head and neck cancer treated by chemo-radiotherapy. Radiother Oncol 2015;116:87–93. https://doi.org/10.1016/j.radonc.2015.06.007.

[9] Hansen CR, Johansen J, Samsøe E, Andersen E, Petersen JBB, Jensen K, et al. Consequences of introducing geometric GTV to CTV margin expansion in DAHANCA contouring guidelines for head and neck radiotherapy. Radiother Oncol 2018;126:43–7. https://doi.org/10.1016/j.radonc.2017.09.019.
[10] Campbell S, Poon I, Markel D, Vena D, Higgins K, Enepekides D, et al. Evaluation of microscopic disease in oral tongue cancer using whole-mount histopathologic techniques: Implications for the management of head-and-neck cancers. Int J Radiat Oncol Biol Phys 2012;82:574–81. https://doi.org/10.1016/j.ijrobp.2010.09.038.
[11] Fleury B, Thariat J, Barnoud R, Buiret G, Lebreton F, Bancel B, et al. Approche anatomopathologique de l'extension microscopique des carcinomes épidermoïdes ORL: implications pour la définition du volume cible anatomoclinique. Cancer/Radiothérapie 2014;18:666–71. https://doi.org/10.1016/j.canrad.2014.04.006.
[12] Ligtenberg H, Jager EA, Caldas-Magalhaes J, Schakel T, Pameijer FA, Kasperts N, et al. Modality-specific target definition for laryngeal and hypopharyngeal cancer on FDG-PET, CT and MRI. Radiother Oncol 2017;123:63–70. https://doi.org/10.1016/j.radonc.2017.02.005.
[13] Yuen PW, Lam KY, Chan ACL, Wei WI, Lam LK. Clinicopathological Analysis of Local Spread of Carcinoma of the Tongue 11The study was supported by a research grant from the University of Hong Kong, grant number 337/048/0014 and 335/048/0081. Am J Surg 1998;175:242–4. https://doi.org/10.1016/S0002-9610(97)00282-1.
[14] Ferreira B, Marques R, Khouri L, Santos T, Sá-Couto P, do Carmo Lopes M. Assessment and topographic characterization of locoregional recurrences in head and neck tumours. Radiat Oncol 2015;10:41. https://doi.org/10.1186/s13014-015-0345-4.
[15] Due AK, Vogelius IR, Aznar MC, Bentzen SM, Berthelsen AK, Korreman SS, et al. Recurrences after intensity modulated radiotherapy for head and neck squamous cell carcinoma more likely to originate from regions with high baseline [18F]-FDG uptake. Radiother Oncol 2014;111:360–5. https://doi.org/10.1016/j.radonc.2014.06.001.
[16] Bayman E, Prestwich RJD, Speight R, Aspin L, Garratt L, Wilson S, et al. Patterns of failure after intensity-modulated radiotherapy in head and neck squamous cell carcinoma using compartmental clinical target volume delineation. Clin Oncol 2014;26:636–42. https://doi.org/10.1016/j.clon.2014.05.001.
[17] Zukauskaite R, Hansen CR, Grau C, Samsøe E, Johansen J, Petersen JBB, et al. Local recurrences after curative IMRT for HNSCC: effect of different GTV to high-dose CTV margins. Radiother Oncol 2018;126:48–55. https://doi.org/10.1016/j.radonc.2017.11.024.
[18] Jager EA, Willems SM, Schakel T, Kooij N, Slootweg PJ, Philippens MEP, et al. Interobserver variation among pathologists for delineation of tumor on H&E-sections of laryngeal and hypopharyngeal carcinoma. How good is the gold standard? Acta Oncol 2016;55:391–5. https://doi.org/10.3109/0284186X.2015.1049661.
[19] Schweinzer K, Kofler L, Bauer J, Metzler G, Breuninger H, Häfner H-M. Cytokeratin AE1/AE3 immunostaining and 3D-histology: improvement of diagnosis in desmoplastic squamous cell carcinoma of the skin. Arch Dermatol Res 2017;309:43–6. https://doi.org/10.1007/s00403-016-1700-5.
[20] Bol GH, Kotte ANTJ, van der Heide UA, Lagendijk JJW. Simultaneous multi-modality ROI delineation in clinical practice. Comput Methods Programs Biomed 2009;96:133–40. https://doi.org/10.1016/j.cmpb.2009.04.008.
[21] Caldas-Magalhaes J, Kasperts N, Kooij N, Van Den Berg CAT, Terhaard CHJ, Raaijmakers CPJ, et al. Validation of imaging with pathology in laryngeal cancer: Accuracy of the registration methodology. Int J Radiat Oncol Biol Phys 2012;82:289–98. https://doi.org/10.1016/j.ijrobp.2011.05.004.
[22] Caldas-Magalhaes J, Kooij N, Ligtenberg H, Jager EA, Schakel T, Kasperts N, et al [The accuracy of target delineation in laryngeal and hypopharyngeal cancer]. Acta Oncol (Madr) 2015;54:1181–7. https://doi.org/10.3109/0284186X.2015.1006401.
[23] Van Cann EM, Rijpkema M, Heerschap A, van der Bilt A, Koole R, Stoelinga PJW. Quantitative dynamic contrast-enhanced MRI for the assessment of mandibular invasion by squamous cell carcinoma. Oral Oncol 2008;44:1147–54. https://doi.org/10.1016/j.oraloncology.2008.02.009.
[24] Becker M, Zbären P, Laeng H, Stoupis C, Porcellini B, Vock P. Neoplastic invasion of the laryngeal cartilage: comparison of MR imaging and CT with histopathologic correlation. Radiology 1995;194:661–9. https://doi.org/10.1148/radiology.194.3.7862960.
[25] Relation T, Dominici M, Horwitz EM. Concise review: an (im)penetrable shield: how the tumor microenvironment protects cancer stem cells. Stem Cells 2017;35:1123–30. https://doi.org/10.1002/stem.2596.
[26] Kitamura R, Toyoshima T, Tanaka H, Kawano S, Kiyosue T, Matsubara R, et al. Association of cytokeratin 17 expression with differentiation in oral squamous cell carcinoma. J Cancer Res Clin Oncol 2012;138:1299–310. https://doi.org/10.1007/s00432-012-1202-6.
[27] Van der Velden LA, Schaafsma HE, Manni JJ, Ruiter DJ, Ramaekers FCS, Kuijpers W. Cytokeratin and vimentin expression in normal epithelium and squamous cell carcinomas of the larynx. Eur Arch Oto-Rhino-Laryngology 1997;254:376–83. https://doi.org/10.1007/BF01642554.
[28] Woolgar JA. Histopathological prognosticators in oral and oropharyngeal squamous cell carcinoma. Oral Oncol 2006;42:229–39. https://doi.org/10.1016/j.oraloncology.2005.05.008.